# Rotograb: Combining Biomimetic Hands with Industrial Grippers using a Rotating Thumb

Arnaud Bersier[1†], Matteo Leonforte[1†], Alessio Vanetta[1†], Sarah Lia Andrea Wotke[1†], Alexander M. Kübler[1] and Robert K. Katzschmann[1*]

***Abstract*— ... Rotograb, a novel tendon-actuated robotic hand with a rotating thumb designed for enhanced dexterity and precision in manipulation tasks. The rotating thumb allows Rotograb to switch between left and right hand mode, and middle mode similar to an industrial gripper. The rotating thumb also supports in-hand manipulation tasks and enables a large workspace. By removing the interior of the links and routing tendons through the center of rolling contact joints, we decouple the bending of different joints, allowing for precise actuation without interference from adjacent movements. The tendon routing for the thumb, designed to not be affected by plate rotation, further contributes to the hand's versatility. Our approach to teleoperation leverages the OAK-D Pro depth camera and Google Mediapipe for real-time hand-tracking, enabling intuitive control over Rotograb by mimicking the user's hand movements. Additionally, we explore the application of reinforcement learning for autonomous object manipulation, demonstrating the hand's capability to adapt and perform complex tasks, such as rotating objects within its grasp. Experimental evaluations highlight Rotograb's effective workspace and its ability to execute a variety of grasps, as illustrated through grasping tasks using objects from the YCB dataset. These results underscore the Rotograbs's potential for sophisticated manipulation tasks, bridging the gap between human-like dexterity and efficient industrial gripper.**

## I. Introduction

### A. Motivation

Integrating robots into daily human life necessitates their interaction with complex surrounding environments. One of the biggest challenges they face is being able to handle objects in a skilled and effective way. This is due to a requirement for multiple degrees of freedom and precise control, essential for dealing with a large variety of objects and tasks.

Developing a gripper to perform a single action can be achieved by optimizing the design for the specific task. However, building a versatile manipulator presents a far more complex challenge. It is tempting to mirror a biomimetic hand, given that the world around us is shaped to be human-friendly. Nevertheless, this is not necessarily the optimal and most effective approach. For instance, a more straightforward single degree of freedom gripper designed like a crane may handle grasping large and heavy objects more efficiently.

In this paper, we attempt to challenge the common conception that humanoid grasp is the only possible approach, proposing a hybrid design that combines the powerful grasp of an industrial gripper with a biomimetic design for tasks that require dexterity.

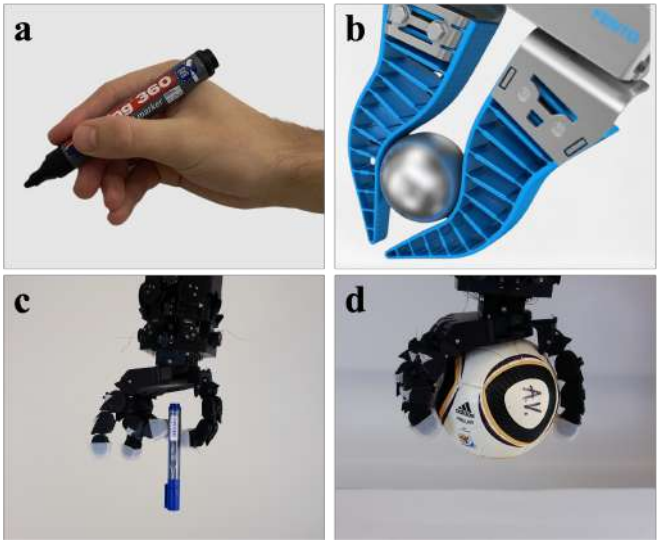


Fig. 1: Example grasps showing the dexterity of a) a human hand and the power grasp capability of b) a industrial gripper, as from Festo SE & Co. KG. Our new robotic gripper Rotograb uses a rotating thumb to combine the dexterity of robotic hands with industrial grippers to achieve c) precision grasps and d) power grasps.

### B. Related Work

The human hand is the most dexterous of all manipulators. It has 21 DoF, excluding the wrist: four in each finger, three for extension and flexion, and one for abduction and adduction. The thumb is more complicated and has five degrees of freedom (DoF). The human hand's complexity ensures versatility and adaptability to a wide range of tasks. Because humans cannot rotate their thumbs to be completely opposed to other fingers, the thenar, a group of three muscles at the base of the thumb, is responsible for bending the palm into a convex shape. This allows humans to grasp large objects. Replicating this degree of freedom in a robotic hand introduces complexity and fragility, making it a less-than-ideal solution.

Nature offers more efficient alternatives when it comes to powerful grasp. For instance, an eagle's grasp can capture prey from above with a safer and stronger grip while flying at high speed. This is achieved through the positioning of one

[1]Soft Robotics Lab, IRIS, D-MAVT, ETH Zurich, Switzerland
† Equal contribution.
∗ Corresponding author: rkk@ethz.ch

finger as opposed to the others. Simple industrial grippers mimic this design with parallel grippers to perform strong and simple grasps.

State-of-the-art robotic manipulators can be categorized into two primary groups: those optimized for pick-and-place operations, resembling industrial-style grippers, and those designed for intricate in-hand manipulations. Standard industrial grippers, such as the ROBOTIQ adaptive gripper [1], typically employ two opposing fingers and optimize the grasping force through strategic design elements and sensor integration, whereas others, like the ROBOTIQ 3-finger Gripper [2], introduce an additional layer of complexity with an extra finger for adaptability. However, these grippers often remain bulky and lack versatility, primarily focusing on simple grasp tasks in industrial settings.

The iRobot-Harvard-Yale Hand [3] enhances versatility with five degrees of freedom (DoF) distributed among its three fingers. This hand showcases a straightforward, durable, and cost-effective design aimed at enhancing functionality. Notably, the gripper is not only proficient in grasping objects but also adept at pinching tasks and even enables a seamless transition from pinching to power grip, introducing the concept of in-hand manipulation. Similarly, the Eagle Shoal [4] offers a low-cost, modular design with rotating fingers for enhanced versatility and expanded range of achievable tasks. The commonality among these grippers is their reliance on three fingers, often in opposition, for better grasping and pinching. However, this configuration appears to limit their manipulation capabilities, and none of them demonstrate the ability to perform intricate in-hand manipulation tasks.

On the opposite end of the spectrum, complex gripper designs, employing numerous actuators and fingers with multiple degrees of freedom excel in in-hand manipulation tasks that range from simple actions like seamlessly transitioning from pinching to grasping to more complex tasks such as flipping a pen or rotating a ball in-hand. Prime examples include the Shunk Hand [5], or the Shadow Hand [6] from Shadow Robotics, which exhibits very high complexity, featuring 20 DC motors, fingers with 4 joints and 3 DoF each, and a thumb with 5 joints and 5 DoF. In general, anthropomorphic hands [5]–[8] delve deeply into mimicking human physiology, by replicating human bones, joints, tendons, and ligaments through tendon-driven mechanisms. Their fabrication and assembly are complex and time-consuming, which makes them expensive.

Conversely, other variants have attempted to balance price and complexity by simplifying the anthropomorphic aspect of the design. Hands such as Carnegie Mellon University's LEAP Hand [9], which uses a simplified design with four fingers or the Allegro Hand [10], based on a design with four fingers and 16 independently actuated joints employ direct actuation with actuators placed directly at the joints. These hands are innovative but tend to be bulkier and compromise compliance.

The state-of-the-art thus shows a clear divide: on one side are the sophisticated and often delicate biomimetic models with high costs and complexity; on the other are the simpler, more robust, and economical industrial-style grippers, which compromise on dexterity and precision. This paper seeks to bridge this gap by proposing a design that synergizes the simplicity and affordability of industrial models with the functional versatility of more complex systems. The proposed design aims to seamlessly perform both pick-and-place tasks and in-hand manipulations, showcasing good performance in both cases.

### C. Contributions

This work contributes to the ongoing research on creating an affordable and versatile robotic manipulator, addressing the trade-offs between complexity, cost, and functionality evident in existing designs. The contributions of this work are:

- A new mechanical design of a robotic hand with a rotating thumb to combine the advantages of biomimetic hands and industrial grippers
- A hollow rolling-contact joint to simplify the joint kinematics
- The demonstration and evaluation of the system, using items from the YCB dataset [11].

## II. Design

Our gripper, called Rotograb aims to fuse the advantages of human hands with industrial grippers. To do so, Rotograb has five fingers, like humans, to mimic and achieve the dexterity of a human hand. All fingers have the same design to simplify modeling and fabrication. While the index, middle, ring, and pinkie are attached to the palm, the thumb is mounted on a plate allowed to rotate around the palm, such that it is possible to switch between different configurations: right hand, left hand, or thumb opposed to the fingers. It allows the hand to switch between "dexterous" grasp and "powerful". The hand has 11 DoF, distributed as follows: two per finger and one for the rotating plate. The hand is mounted with a $10\,\mathrm{deg}$ angle with respect to the horizontal wrist plane, where the 11 servo actuators are located. Figure 2 shows the details of Rotograb as well as its CAD design. In the following, we will explain the design in more detail.

### A. Fingers

All fingers follow the same design. Each finger is made of four links: the base, the lower and upper link, and the tip (Figure Figure 3). The links are connected by three rolling contact joints. In particular, they are held together by four separate ligaments attached in alternating directions (top and bottom side of the finger) to have symmetric compliance along the lateral plane. Rolling contact joints minimize friction and provide some lateral compliance to the finger. Moreover, when subject to exceeding stress, they pop instead of breaking.

The sagittal section (2D lateral view) of the finger is shown in Figure Figure 4 shows the tendon routing in detail. Each part of the finger is made from a combination of a rectangle and two half circles with the same radius.

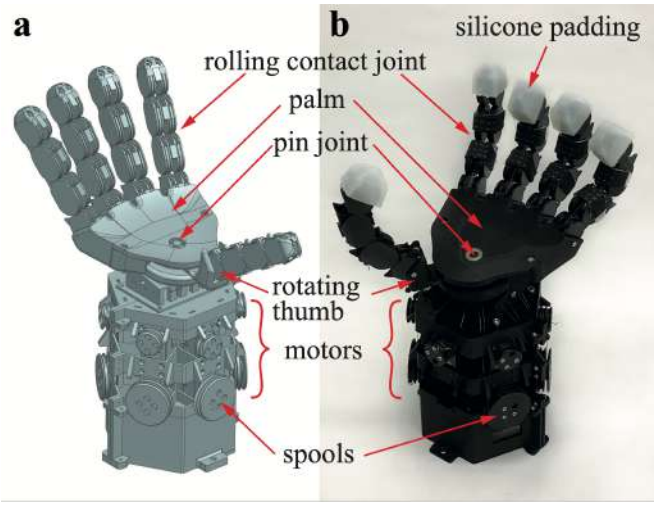


Fig. 2: a) CAD model of Rotograb with five fingers, including the rotating thumb, and the actuation tower below the wrist with motors and spools. b) Assembled 3d-printed Rotograb with silicon padding for increased contact friction.

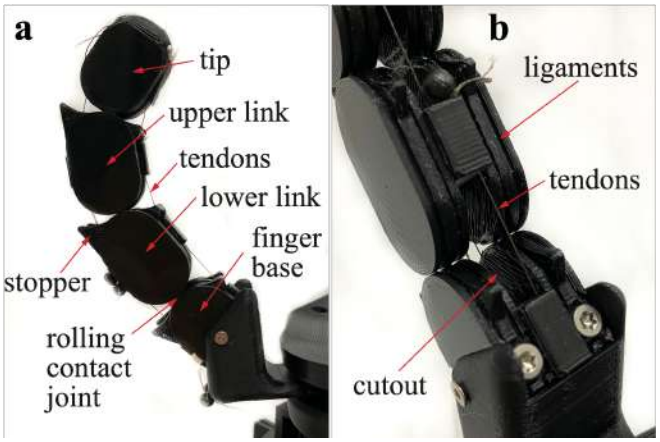


Fig. 3: a) Side view of a finger, specifically the thumb. All fingers have the same design. The finger consists of a finger base and three links (lower links, upper link, and tip). The links are connected by rolling-contact joints and actuated through tendons. Mechanical stoppers limit the movement. b) Close-up of the rolling contact joint with tendons and ligaments. The cut-out in the center of the rolling-contact joint simplifies the finger kinematics.

The movement achieved by the rolling contact joint results from two simultaneous rotations: the 'virtual' rotation around the axis of the upper circle of the bottom link and the 'real' rotation around the axis of the lower circle of the upper link. The two rotations are coupled by the ligaments, and since the radii are equal, they have the same amplitude.

The base of the finger is attached to the palm (or to the rotating plate) at a $45\,\mathrm{deg}$ angle. Joint 1 allows a backward rotation of the finger up to $-45\,\mathrm{deg}$ (flat position), while joints 2 and 3 can only flex forward. The maximum inward flexing angle is $90\,\mathrm{deg}$ for all joints. Mechanical stoppers enforce the range of motion.

Tendon calculations of the tendon routing are complex for rolling contact joints because the contact point from which the tendon applies a force to the link changes with the angle. To simplify the problem, we cut out the internal part of each link is. This results in a simplified control and kinematics with a minimal impact on robustness, as discussed in Section III.

The tips of all fingers are wrapped in a case of silicone. This wrapping increases the friction coefficient to grasp objects more easily and helps for a higher degree of softness when dealing with delicate objects.

### B. Rotating Thumb

The thumb is designed the same way as the other fingers and is fixed on a rotating plate. The plate is attached to the center of the palm through a pin joint with a bearing to minimize the friction. The resting position is shown in Figure Figure 2.a). In this configuration, it acts in the opposite direction to the other fingers.

The plate is actuated using two tendons that pull on the right and left side, respectively, and it can move from $-65\,\mathrm{deg}$ to $+65\,\mathrm{deg}$. The tendons that actuate the thumb itself are routed through the inside of the plate. To decouple the flexion and extension of the thumb from the rotation of the plate, the thumb tendons are routed as close as possible to the axis of rotation of the plate. This ensures that the plate angle does not affect the tendon length of the thumb.

### C. Wrist

The hand is mounted with an angle of $10\,\mathrm{deg}$ with respect to the plane orthogonal to the axis of the wrist. This choice allows the hand to grasp objects from above and operate in limited space, similar to the eagle's talon. The hand orientation minimizes the torque applied to the wrist since most of the gravitational force is applied along the axis of the wrist.

### D. Actuation and Tendon Routing

Each tendon is attached to a servo-motor through a spool. The tendons are routed inside the wrist up to the fingers. Inside the finger, the routing follows human tendons' routing: two flexor and two extensor tendons (Figure Figure 4.a). The application point of tendons, where they pull the links from, is always chosen to be on the extremity of the diameter the link's circles.

The tendons are routed through the cut-out part of the links. A key benefit of this is that the distance between the centers of rotation of two adjacent links is constant (e.g., segment $O_1O_1'$ in Figure Figure 5.a). In order to decouple the actuation of the lower and upper parts of the finger, we route the tendons for the joints 2 and 3 through the centers of rotation of joint 1 and 2, respectively. This way, the tendon length of the upper joints will not be affected by the actuation angle of joint previous joints (see Section Section III for more details).

Each finger is actuated by two motors. One controls joint 1, the other controls the coupled two upper joints 2 and 3.

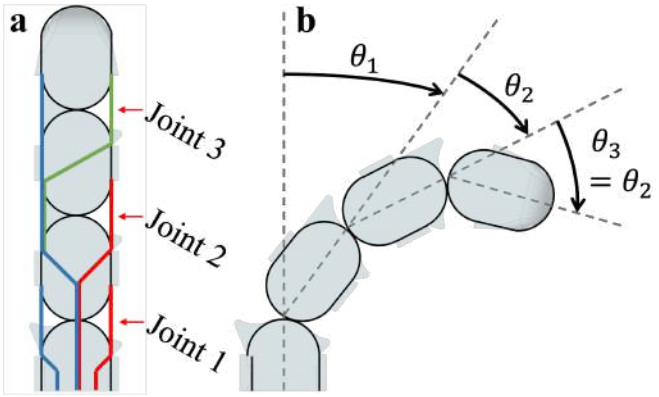


Fig. 4: a) CAD side view of the tendon routing inside the finger with three joints. Flexor tendons are drawn in red, extensor tendons are blue, while the green tendon couples the flexion of joints 2 and 3. b) Illustration of the joint angles of a finger, with joint 2 and 3 being coupled.

Each motor is attached to two spools, one for the flexor and one for the extensor tendon. Since the amount of tendon pulled differs for the flexor and the extensor for the upper coupled joints, the spools have different radii with a constant ratio. The extensors for joint 2 and joint 3 are combined in one tendon. This combination makes the single extensor to increase/decrease twice as much as the corresponding flexor of joint 2. Choosing double the spool radius for the extensor than for the flexor simplifies the kinematic calculations to the ones introduced in the next section.

## III. Kinematics

The hand is fully tendon-actuated through 11 servo-motors positioned in the wrist. We made three design choices to simplify the kinematic calculations: First, The inside of the links is removed. Therefore, flexor and extensor are routed through the center of of the rolling contact joint. This decouples the bending of different joints. A bending in lower joint (e.g., joint 1) does not deflect the tendon actuation a upper joint (e.g., joint 2). Therefore, we can calculate the deflection only at the actuated joint. Any non-linearities of bending tendons is bypassed. Second, the tendons of the thumb are routed through the center of rotation of the plate. This way the rotation of the plate does not affect the tendon lengths of flexors or extensors in the thumb. Third, the choice of spool radii takes occuring differences in tendon length increase & decrease into account.

### A. Fingers

Each individual finger has two actuated DoFs with the same geometry and tendon routing. We use a simplified 2D problem to compute the finger kinematics, which is equal for all fingers.

In order to actuate the robotic hand, a desired joint angle $\theta$ needs to be translated into a change in tendon length $\Delta l$. Divided by the radius of the spool, this results in the motor rotation needed to achieve the desired joint angle. Since the tendon length routed through the palm and through the interior cut-out of the links stays constant, the only varying lengths are found between consecutive links, denoted as $\vec{l}_{P_i P_i'}$.

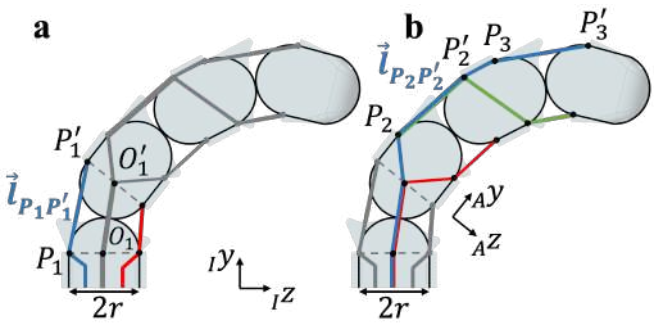


Fig. 5: 2D-model of the finger kinematics: a) Joint 1 modeled with flexor (red) and extensor (blue) tendons. b) Joints 2 and 3 with combined flexor (red) and extensor (blue) tendons and the coupled flexor tendon (green).

The equations for the kinematics of the finger are introduced by first looking at joint 1 using the model depicted in Figure Figure 5.a. The points $O_1$ and $O_1'$ are the centers of the virtual and real rotations, respectively. The distance between these points stays the same as a result of the design features mentioned in the beginning of this section. The points $P_1$ and $P_1'$ are the exit and entry points of the extension tendon, respectively. For the calculations we only consider the length between these two points.

The calculation of the tendon length vector ${}_I l_{P_1 P_1'}$ can be simplified to the following equations:

$$\begin{aligned} {}_I l_{P_1 P_1'}(\theta_1) &= \begin{bmatrix} {}_I l_y(\theta_1) \\ {}_I l_z(\theta_1) \end{bmatrix} \\ &= \begin{bmatrix} r \cdot \sin\theta_1 + 2r \cdot \cos\frac{\theta_1}{2} \\ r \cdot (1 - \cos\theta_1) + 2r \cdot \sin\frac{\theta_1}{2} \end{bmatrix} \end{aligned} \tag{1}$$

The final change in tendon length $\Delta l(\theta_1)$ is calculated by

$$\Delta l(\theta_1) = \| {}_I l_{P_1 P_1'}(\theta_1) \| - \| {}_I l_{P_1 P_1'}(\theta_{1,init}) \| \tag{2}$$

where $\theta_1$ is the desired joint angle chosen for joint 1, and $\theta_{1,init}$ is the calibration angle. In the case of joint 1 it holds that $\theta_{1,init} = -45\,\text{deg}$. To move the finger, the change in tendon length is added to the extensor length and subtracted from the flexor length.

Thanks to the design choices the calculations for joint 2 are done analogously as for joint 1. As seen in Figure Figure 5.b, for joint 2 we use the reference frame $A$ and apply the same calculations to obtain the tendon length vector ${}_A l_{P_2 P_2'}$ and the change in tendon length $\Delta l(\theta_2)$ depending on the desired joint angle $\theta_2$ and calibration angle of joint 2, $\theta_{2,cal} = 0\,\text{deg}$

The flexion or extension of joint 3 happens simultaneously to the one of joint #2 since the coupling connects the movements directly.

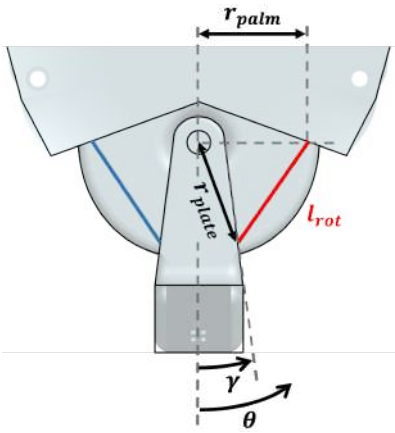


Fig. 6: 2D model of the rotating thumb. $\theta$ indicates the state of the thumb's rotation, with $\theta = 0$ indicating the middle position of the thumb.

### B. Rotating Thumb

For the tendon length calculation of the rotating thumb, the calculations can also be simplified to a 2D problem, as seen in Figure Figure 6. Knowing the dimensions $r_{palm}$, $r_{plate}$, and $\gamma$, the tendon length $l_{rot}$ is computed using the cosine theorem:

$$l_{rot}(\theta) = \sqrt{r_{palm}^2 + r_{plate}^2 - 2r_{palm}r_{plate}\cos\left(\frac{\pi}{2} - (\theta + \gamma)\right)} \tag{3}$$

The change in tendon length is then computed by

$$\Delta l_{rot}(\theta) = l_{rot}(\theta) - l_{rot}(\theta_0) \tag{4}$$

where for calibration purposes we choose $\theta_0 = 0$. Due to the symmetry of the design, the length of the left tendon is increasing by the same amount as the length of the right tendon is decreasing.

The tendon routing of the thumb goes through the axis of rotation of the plate, designed to decouple the hinge joint in the palm and the flexion/extension of the thumb. The calculation for the tendons of the thumb, thus, can be done analogously to the one for the other fingers (see Section Section III-A).

## IV. Control

### A. Teleoperation

Rotograb can be operated through teleoperation. The users' hand movements serve as the input which is then mapped to the gripper. We used an OAK-D Pro (Luxions) depth camera to capture the movements of a human user. The camera tracked the user's hand, and then landmarks are extracted using the hand-tracking model from Google Mediapipe [12]. The input angles of the human hand are mapped for each actuated joint to the robotic gripper. For the index, middle, ring, and pinky finger the mapping is done directly.For the thumb, we detect of the human is showing the left or the right and and consequently switch the mode of the hand. All the angles are scaled and tuned to achieve smooth operation of the robotic hand over its full workspace, especially for the workspace of the rotating thumb.

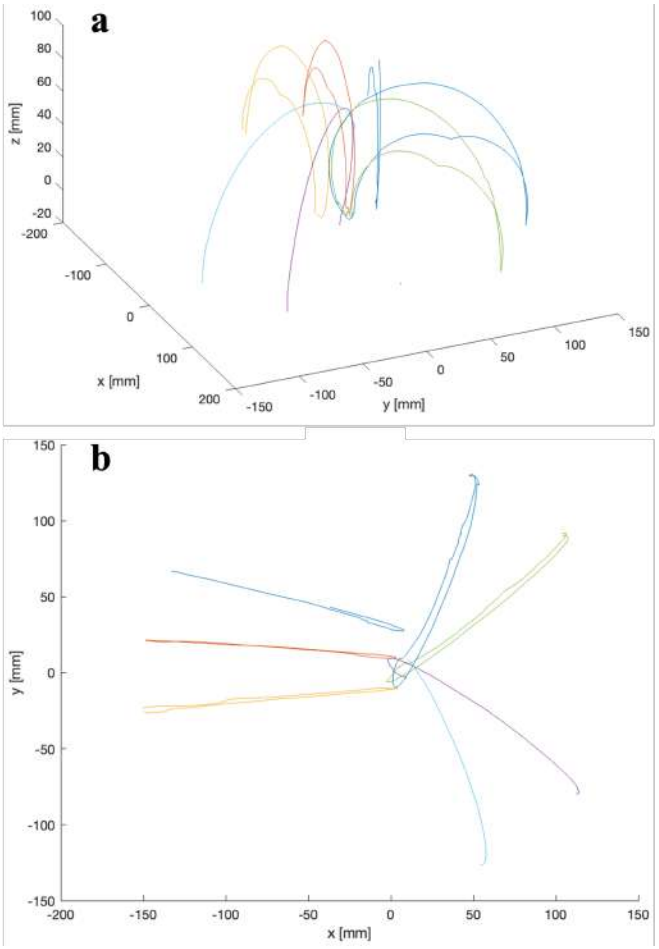


Fig. 7: Workspace analysis of all finger tips. The plots indicate the outer boundary of the finger tip motions in a) 3D and b) projected onto the the x-y-plane (orthogonal to the center line of Rotograb's actuation tower. The fingers are indicated in the plot, and the thumb is shown in left, middle, and right position.

### B. Reinforcement Learning

We also implemented a reinforcement learning to autonomously rotate objects in the hand. We follow a similar pipeline to the ball rolling introduced by Toshimitsu et. al. [14]. We also trained to roll a ball on the palm in two opposite directions, but also tested it with other objects. We used the GPU-based simulators IsaacGym [15] to simulate thousands of robots in parallel. All the dexterous manipulation policies were learned in around 40 minutes on a single NVIDIA GeForce RTX 3060 GPU. Each training is 2000 epochs long and involves 4096 simultaneous environments. We used the PPO algorithm [16] from the open-source repository RL-Games [17]. The reward specific for the ball rotation is the object rotation velocity reward, which returns the maximum reward when the absolute rotational velocity around the x-axis is between 1 and 3 $rad/s$, and linearly

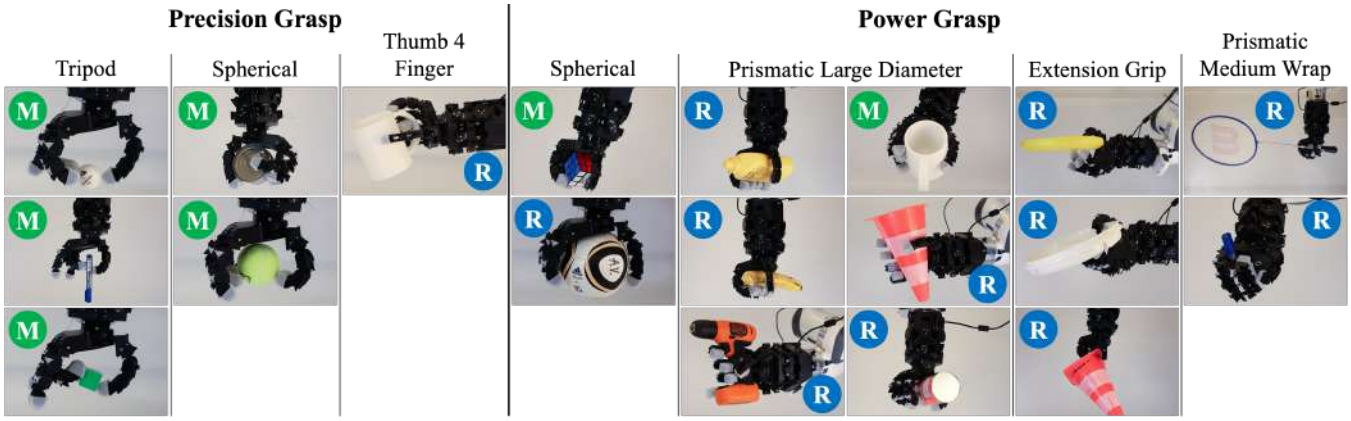


Fig. 8: Rotograb grasping different objects from the YCB dataset [11] with precision or power grasps. The grasp are categorized by the grasp taxonomy introduced by Mark R. Cutkosky [13]. We indicate the position of the thumb by "L", "M", or "R" meaning left, middle, or right position, respectively.

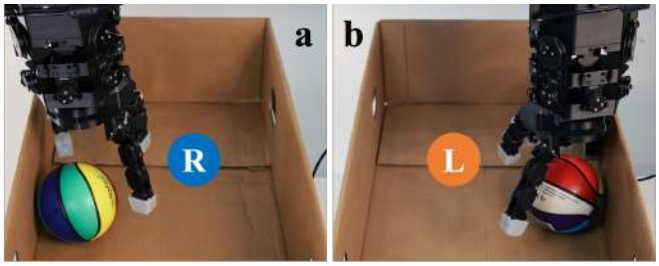


Fig. 9: Showcase of the ambidexterity of Rotograb. It grasps a ball which is constrained by a close wall. a) The wall is left of the ball. Rotograb can grasp in ball with the thumb on the right side. b) The wall is right of the ball. Rotograb can grasp in ball with the thumb on the left side.

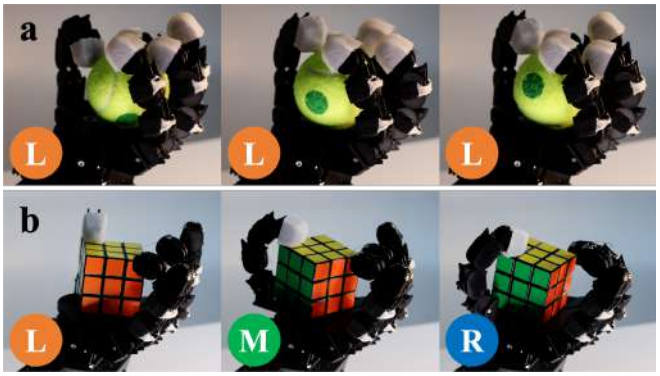


Fig. 10: Showcase of the in-hand manipulation capabilities of Rotograb, based on Reinforcement Learning. a) Rotograb roll a ball with the thumb being on the left side and the other four fingers to most of the ball rolling. b) Rotograb re-orients a rubiks cube using its rotating thumb.

decreases outside of this region. The sign of $\omega x$ in the reward formula can be flipped to reverse the desired direction of rotation.

To compensate for the inaccuracy of the physics engine and to make the policy more robust to overcome the sim2real gap, we applied domain randomization to the physics properties. Gaussian or uniform noise was added to observations, actions, damping and stiffness of the tendons and the joints, joint range of motion, mass and friction of the robot and object, and object scale.

## V. Experimental Evaluation

### A. Workspace

To quantify how Rotograb can reach finger tip positions in its workspace, we analyzed the finger tip motions in a motion capture system (Qualisys). **??** shows the workspace of the different fingers in the 3D space and projected to the x-y plane. We find that the rotating thumb captures a large workspace opposed to the other fingers. This shows that our design philosophy can indeed capture different states from industrial gripper to dexterous hands with ambidexteriy. We also see that each finger captures a similar workspace. For future improvements, we will add aduction and abduction to all fingers to close the workspace gap between the fingers.

### B. Object Grasping

To assess the grasping capabilities, Rotograb was tested with a set of objects chosen from the YCB benchmark dataset [11], [18]. The objects used in the test are listed in Table **??**. We find that Rotograp can grasp small, delicate objects like a pingpong ball or a pen, as well as large power grasp objects such as a handball or pylons. Depending on the object, Rotograp switches between a hand state (thumb on the left or right side) or a industrial gripper state (thumb in middle position).

### C. Ambidexterity

To evaluate the ambidexterity capabilities of Rotograb, we placed a ball in two different positions in a box: next to the left wall and next to the right wall. The grasping procedure is therefore restricted by the walls of the box depending on

the position of the ball. The success of grasping the ball in each position is surveyed for left and right thumb position.

As shown in Figure Figure 9 the two hand modes succeed for different positions of the ball. It highlights that the design of Rotograb allows to grab objects in different situations. The left hand mode is particularly useful in case the grasping is restricted by a wall to the left of the object while the right hand mode is usable in configurations where the object is blocked by a wall to the right. This shows that the Rotograb can access objects in confined spaces without a change in rotation or orientation of the robotic arm it is mounted on.

### D. In-Hand Manipulation

In-hand reorientation is a crucial capability for a robot manipulator to execute tasks in real-world scenarios. It necessitates precise control and being highly sensitive to design choices. To demonstrate this concept, we present two experiments that underscore the benefits of our rotating thumb. As illustrated in Figure **??**, the experiments involve rotating a tennis ball around the x-axis and a Rubik's cube around the z-axis. The tennis ball, due to its simpler and more symmetric shape, allows for an autonomously learned policy via Reinforcement Learning on Isaac Gym. This policy involves the thumb alternating between a lateral and a central configuration. On the actual hardware, the ball rotates at an approximate speed of 5.45 rounds per minute.

For the Rubik's Cube, the policy was hard-coded to emphasize the pivotal role of the thumb. The rotation around the palm proves to be particularly useful for rotating objects around the palm's axis when the abduction movement of other fingers is not feasible. The thumb rotates by pushing the cube's edges, while the other fingers provide counter torque, enabling the rotation. When tested on the actual hardware, the cube rotates at an approximate speed of 5.62 rounds per minute.

## VI. Conclusion

Our work presents a novel type of robotic gripper, called Rotograb, which combines the advantage of humanoid hands and the strength of industrial grasp. The movable thumb, significantly enhances grip strength, particularly for large objects, while maintaining Rotograb's dexterity for small and delicate objects. We introduce a new type of rolling-contact joint which has a cut-out in the center to simplify the finger kinematics.

Our workspace analysis underlines the potential of the rotating thumb. However, adding aduction and abduction to the fingers will improve the workspace in the future. We showcase its capabilities by manipulating a large set of objects, from small pens and ping-pong balls, to pillons and balls. The movable thumb also allows for ambidexterity to perform tasks as a left, or a right hand. We integrated teleoperation control as well as a reinforcement learning approach. With the latter, Rotograb was able to in-hand manipulate different objects such as a tennis ball and a rubiks cube.

In a next step, we want to increase the robustness of Rotograp and make sligher fingers with aduction and abduction. We will improve control and teleoperation focusing on the mapping between the user input and Rotograp. The differences in shape and size between the human hand and the robotic hand make the mapping particularly challenging. Furthermore, we want to undertake more quantitive manipulaiton tests to analyze and improve Rotograp'c capabilities.

## Acknowledgment

The authors thank the team of the Real-World-Robotics class (*www.rwr.ethz.ch*) at ETH Zurich which served as a starting point for this project.

## References

[1] ROBOTIQ. "Robotiq gripper." (), [Online]. Available: https://robotiq.com/fr/produits/main-adaptative-a-2-doigts-hand-e.

[2] ROBOTIQ. "Robotiq hand." (), [Online]. Available: https://robotiq.com/products/3-finger-adaptive-robot-gripper.

[3] L. U. Odhner, L. P. Jentoft, M. R. Claffee, *et al.*, "A compliant, underactuated hand for robust manipulation," *The International Journal of Robotics Research*, vol. 33, no. 5, pp. 736–752, 2014. eprint: https://doi.org/10.1177/0278364913514466.

[4] T. Wang, Z. Geng, B. Kang, and X. Luo, "Eagle shoal: A new designed modular tactile sensing dexterous hand for domestic service robots," in *2019 International Conference on Robotics and Automation (ICRA)*, 2019, pp. 9087–9093.

[5] S. S.
bibinitperiod C. KG. "Shunk hand." (), [Online]. Available: https://schunk.com/us/en/gripping-systems/special-gripper/svh/c/PGR_3161.

[6] S. R. Company. "Shadow hand." (), [Online]. Available: https://www.shadowrobot.com/dexterous-hand-series/.

[7] B. J. Tasi, M. Koller, and G. Cserey, "Design of the anatomically correct, biomechatronic hand," *CoRR*, vol. abs/1909.07966, 2019. arXiv: 1909.07966.

[8] Z. Xu and E. Todorov, "Design of a highly biomimetic anthropomorphic robotic hand towards artificial limb regeneration," in *2016 IEEE International Conference on Robotics and Automation (ICRA)*, 2016, pp. 3485–3492.

[9] K. Shaw, A. Agarwal, and D. Pathak, *Leap hand: Low-cost, efficient, and anthropomorphic hand for robot learning*, 2023. arXiv: 2309.06440 [cs.RO].

[10] W. Robotics, *Allegro hand: Highly adaptive robotic hand for r&d*, 2023.

[11] B. Calli, A. Singh, A. Walsman, S. Srinivasa, P. Abbeel, and A. M. Dollar, "The ycb object and model set: Towards common benchmarks for manipulation research," in *2015 International Conference on Advanced Robotics (ICAR)*, 2015, pp. 510–517.

[12] C. Lugaresi, J. Tang, H. Nash, *et al.*, "Mediapipe: A framework for perceiving and processing reality," in *Third workshop on computer vision for AR/VR at IEEE computer vision and pattern recognition (CVPR)*, vol. 2019, 2019.

[13] M. R. Cutkosky *et al.*, "On grasp choice, grasp models, and the design of hands for manufacturing tasks.," *IEEE Transactions on robotics and automation*, vol. 5, no. 3, pp. 269–279, 1989.

[14] Y. Toshimitsu, B. Forrai, B. G. Cangan, *et al.*, *Getting the ball rolling: Learning a dexterous policy for a biomimetic tendon-driven hand with rolling contact joints*, 2023. arXiv: 2308.02453 [cs.RO].

[15] V. Makoviychuk, L. Wawrzyniak, Y. Guo, *et al.*, "Isaac gym: High performance GPU based physics simulation for robot learning," Nov. 2021.

[16] J. Schulman, F. Wolski, P. Dhariwal, A. Radford, and O. Klimov, "Proximal policy optimization algorithms," Jul. 2017. arXiv: 1707.06347 [cs.LG].

[17] D. Makoviichuk and V. Makoviychuk, *Rl-games: A high-performance framework for reinforcement learning*, https://github.com/Denys88/rl_games, May 2021.

[18] AUTHOR???? "Ycb benchmarks." (), [Online]. Available: https://www.ycbbenchmarks.com/object-set/.